Science, Trieste, Italy, 2015); http://pos.sissa.it/archive/conferences/215/037/AASKA14_037.pdf.
27. X. Siemens, J. Ellis, F. Jenet, J. D. Romano, *Class. Quantum Gravity* **30**, 224015 (2013).
28. S. W. Hawking, *Astrophys. J.* **145**, 544 (1966).
29. P. B. Demorest *et al.*, *Astrophys. J.* **762**, 94 (2013).

ACKNOWLEDGMENTS

We thank the observers, engineers, and Parkes Observatory staff members who have assisted with the observations reported in this paper. We thank R. van Haasteren for assistance with the use of the code *piccard*, E. Thomas for comments on the manuscript, and I. Mandel for discussions on model selection. The Parkes radio telescope is part of the Australia Telescope National Facility, which is funded by the Commonwealth of Australia for operation as a National Facility managed by CSIRO. The PPTA project was initiated with support from R.N.M.'s Australian Research Council (ARC) Federation Fellowship (grant FF0348478) and from CSIRO under that fellowship program. The PPTA project has also received support from ARC through Discovery Project grants DP0985272 and DP140102578. N.D.R.B. acknowledges support from a Curtin University research fellowship. G.H. and Y.L. are recipients of ARC Future Fellowships (respectively, grants FT120100595 and FT110100384). S.O. is supported by the Alexander von Humboldt Foundation. R.M.S. acknowledges travel support from CSIRO through a John Philip Award for excellence in early-career research. The authors declare no conflicts of interest. Data used in this analysis can be accessed via the Australian National Data Service (www.ands.org.au).

SUPPLEMENTARY MATERIALS

www.sciencemag.org/content/349/6255/1522/suppl/DC1
Supplementary Text
Figs. S1 to S2
Tables S1 to S8
References (*30*–*54*)

26 March 2015; accepted 12 August 2015
10.1126/science.aab1910

BIOCATALYSIS

Conversion of alcohols to enantiopure amines through dual-enzyme hydrogen-borrowing cascades

Francesco G. Mutti,[1,2]*† Tanja Knaus,[2]† Nigel S. Scrutton,[2] Michael Breuer,[3] Nicholas J. Turner[1]*

α-Chiral amines are key intermediates for the synthesis of a plethora of chemical compounds at industrial scale. We present a biocatalytic hydrogen-borrowing amination of primary and secondary alcohols that allows for the efficient and environmentally benign production of enantiopure amines. The method relies on a combination of two enzymes: an alcohol dehydrogenase (from *Aromatoleum* sp., *Lactobacillus* sp., or *Bacillus* sp.) operating in tandem with an amine dehydrogenase (engineered from *Bacillus* sp.) to aminate a structurally diverse range of aromatic and aliphatic alcohols, yielding up to 96% conversion and 99% enantiomeric excess. Primary alcohols were aminated with high conversion (up to 99%). This redox self-sufficient cascade possesses high atom efficiency, sourcing nitrogen from ammonium and generating water as the sole by-product.

Amines are among the most frequently used chemical intermediates for the production of active pharmaceutical ingredients, fine chemicals, agrochemicals, polymers, dyestuffs, pigments, emulsifiers, and plasticizing agents (*1*). However, the requisite amines are scarce in nature, and their industrial production mainly relies on the metal-catalyzed hydrogenation of enamides (i.e., obtained from related ketone precursors). This process requires transition metal complexes, which are expensive and increasingly unsustainable (*2*). Moreover, the asymmetric synthesis of amines from ketone precursors requires protection and deprotection steps that generate copious amounts of waste. As a consequence, various chemical processes for the direct conversion of alcohols into amines have been developed during the past decade. The intrinsic advantage of the direct amination of an alcohol is that the reagent and the product are in the same oxidation state; therefore, theoretically, additional redox equivalents are not required. However, many of these methods have low efficiency and high environmental impact (e.g., Mitsunobu reaction) (*3*). The amination of simple alcohols such as methanol and ethanol via heterogeneous catalysis requires harsh conditions (>200°C), and more structurally diverse alcohols are either converted with extremely low chemoselectivity or not converted at all (*4*). Furthermore, most of the work in this field involves nonchiral substrates, whereas 40% of the commercial optically active drugs are chiral amines (*2*). Increasingly, biocatalytic methods are applied for the production of optically active amines [e.g., the lipase-catalyzed resolution of racemic mixtures of amines or the ω-transaminase process; a recent example uses an engineered enzyme applied to the industrial manufacture of the diabetes medication Januvia (sitagliptin)] (*5*–*7*).

Multistep chemical reactions in one pot avoid the need for isolation of intermediates and purification steps. This approach offers economic as well as environmental benefits, because it eliminates the need for time-consuming intermediate work-ups and minimizes the use of organic solvents for extraction and purification as well as energy for evaporation and mass transfer (*8*). As a consequence, cascade reactions generally possess elevated atom efficiency and potentially lower environmental impact factors (*9*). The major challenge is to perform cascade reactions wherein an oxidative and a reductive step are running simultaneously. Even more challenging is to carry out a simultaneous interconnected redox-neutral cascade wherein the electrons liberated in the first oxidative step are quantitatively consumed in the subsequent reductive step [(*8*); for a recent detailed study, see (*10*)]. This concept is the basis for the hydrogen-borrowing conversion of alcohols (primary or secondary) into amines. The reducing equivalents (i.e., hydride) liberated in the first step—the oxidation of the alcohol to the ketone—are directly consumed in the second interconnected step—reductive amination of the ketone.

A number of chemocatalytic hydrogen-borrowing methods have recently been developed using ruthenium as well as iridium catalysts (*11*, *12*). However, the required reaction conditions (e.g., high catalyst and cocatalyst loading, low substrate concentration, moderate chemoselectivity, moderate or total lack of stereoselectivity, the requirement of an excess of substrate, and stringent temperature and elevated pressure requirements) complicate the application of these methods on a large scale (*13*). Another recently developed hydrogen-borrowing chemical method involves the stoichiometric use of Ellman's enantiopure sulfinamide auxiliary as the nitrogen donor in combination with a Ru-Macho catalyst (*14*). Besides the requirement of the expensive chiral auxiliary, the maximum diastereomeric excess was 90%. A reported biocatalytic hydrogen-borrowing amination of alcohols combining three enzymes—a ω-transaminase (ωTA), an alcohol dehydrogenase (ADH), and the alanine dehydrogenase from *Bacillus subtilis* (AlaDH)—also lacks efficiency because of the requirement for at least 5 equivalents of L- or D-alanine as the sacrificial amine donor and also as a result of the lower conversion and chemoselectivity for the amination of secondary alcohols (*15*, *16*). Another redox-neutral biocatalytic cascade was applied for the deracemization of mandelic acid to enantioenriched L-phenylglycine. However, the method was limited to the conversion of this specific α-hydroxy acid (*17*).

Here, we present a highly enantioselective catalytic hydrogen-borrowing amination of primary

[1]School of Chemistry, University of Manchester, Manchester Institute of Biotechnology, Manchester M1 7DN, UK. [2]Manchester Institute of Biotechnology, Faculty of Life Sciences, University of Manchester, Manchester M1 7DN, UK. [3]BASF SE, White Biotechnology Research, GBW/B-A030, 67056 Ludwigshafen, Germany.
***Corresponding author. E-mail: nicholas.turner@manchester.ac.uk (N.J.T.); f.mutti@uva.nl (F.G.M.)** †Present address: Van 't Hoff Institute for Molecular Sciences, University of Amsterdam, Science Park 904, 1098 XH Amsterdam, Netherlands.

as well as secondary alcohols that requires only two biocatalysts, namely an ADH and an amine dehydrogenase (AmDH) (Fig. 1). The redox self-sufficient cycle uses ammonium ion/ammonia as the source of the nitrogen and generates only water as the by-product. The cascade requires only catalytic quantities of a nicotinamide coenzyme that shuttles hydride from the oxidative step to the reductive step. The method has been successfully applied to amination of optically active secondary alcohols with inversion of configuration, amination of the corresponding enantiomeric secondary alcohols with retention of configuration, asymmetric amination of racemic secondary alcohols, and amination of primary alcohols.

Initially, we examined the catalytic activity of the amine dehydrogenase variant that was recently obtained by protein engineering of the wild-type phenylalanine dehydrogenase from *B. badius* (Ph-AmDH) (*18*, *19*). The substrate scope of the Ph-AmDH variant K78S-N277L for the conversion of a broad range of ketone substrates has not been reported; only the reductive amination of *para*-fluorophenylacetone (**2b**) was previously described, using glucose and glucose dehydrogenase (GDH) for cofactor regeneration, and very recently three other ketones were also tested (*20*). Hence, the Ph-AmDH variant K78S-N277L was expressed and purified as histidine (His)–tagged protein. The activity of the enzyme was initially studied using **2b** as the test substrate in ammonium buffer systems with a range of different counterions (chloride, sulfate, acetate, phosphate, borate, citrate, oxalate, and formate). The pH was also varied from 4 up to 11.5, depending on the ammonium buffer used (fig. S5). The highest catalytic activity was observed at pH 8.2 to 8.8, whereas the optimal buffer was ammonium chloride. In contrast, previous studies with this enzyme were carried out at pH 9.6 (*18*). Reductive amination of **2b** (20 mM) was carried out at varying concentrations of NH_4Cl/NH_3 buffer at pH 8.7 using GDH and glucose for cofactor regeneration. Quantitative conversion (>99%) was achieved after 12 hours using ~0.7 M ammonium buffer (table S1 and fig. S6).

ADHs have been extensively used in biocatalysis for the interconversion of ketones and alcohols, and hence a wealth of data is available for these enzymes (*21*). Because of the dependence of Ph-AmDH on nicotinamide adenine dinucleotide (oxidized form; NAD) as cofactor, we searched for suitable stereocomplementary NAD-dependent secondary ADHs that might exhibit high stability and activity toward a wide range of secondary alcohols at pH >8.5 as well as tolerance of high concentrations of ammonium ions. The NAD-dependent Prelog ADH from *Aromatoleum aromaticum* (AA-ADH, previously named as denitrifying bacterium strain EbN1; PDB 2EW8 and 2EWM) (*22*) and an engineered anti-Prelog ADH from *Lactobacillus brevis* (LBv-ADH; PDB 1ZK4 for the wild-type enzyme) were selected for this study (*23*–*25*). Analysis of the crystal structures of the ADHs with bound NAD(P)H (reduced NAD phosphate) as well as previous docking studies (i.e., substrate bound to the enzyme) revealed that the active sites of AA-ADH and LBv-ADH possess a very similar amino acid arrangement, but in an inverted conformation. In particular, a tyrosine residue (Tyr^{93} for AA-ADH, Tyr^{189} for LBv-ADH) is crucial for the stereoselectivity, as it protrudes into the active site and forces the substrates to bind with the larger group in the opposite direction. This Tyr residue is in a mirror-image position in the active site of the two ADHs (*22*, *25*).

The amination of alcohol substrate (*R*)-**1a** (20 mM) was carried out initially by combining a crude cell extract of LBv-ADH with purified His-tagged Ph-AmDH in the presence of catalytic NAD^+ [1 mM; 5 mole percent (mol %)] and in the presence of buffer systems ranging from pH 7 to 8.7. Although formation of the amine product (*R*)-**3a** was observed, the maximum conversion was 6%. In particular, accumulation of the ketone intermediate **2a** was observed (from 61% to 97%; table S2). However, under these conditions, the concentration of ketone **2a** cannot exceed the concentration of the cofactor NAD^+ (1 mM), and hence the accumulation of high levels of **2a** was attributed to the presence of at least one NAD oxidase from the host organism (*Escherichia coli*) used for the expression of the ADH, as previously observed by other groups (*26*). The NADH oxidase competed

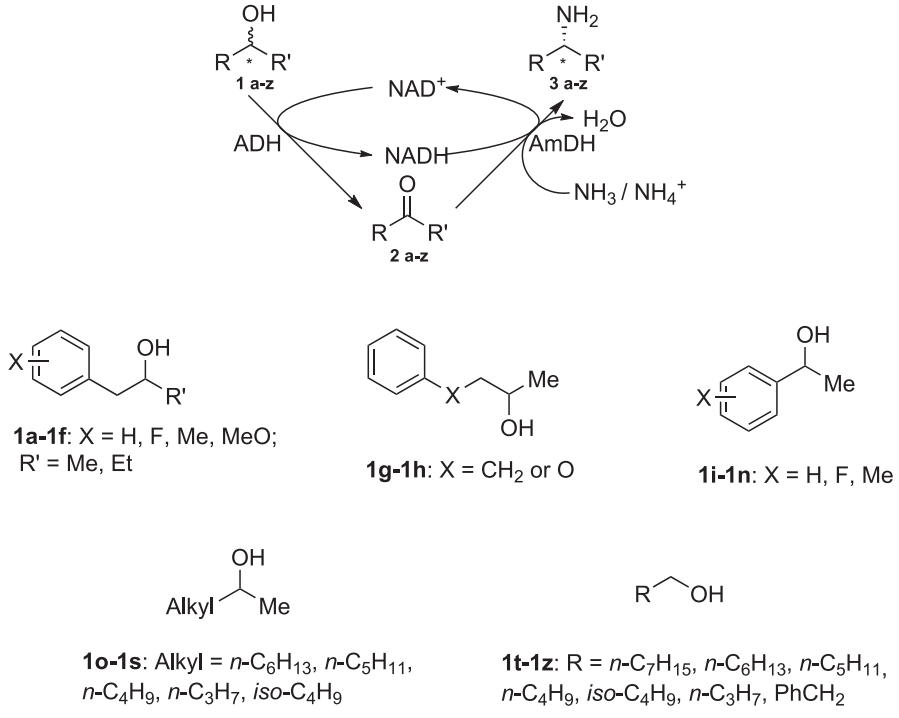

Fig. 1. Two-enzyme cascade for the hydrogen-borrowing amination of alcohols. In the first oxidative step, the Prelog AA-ADH and the anti-Prelog LBv-ADH were applied for the oxidation of the (*S*)- and (*R*)-configured alcohol substrates, respectively. The AmDHs used in this study afforded the (*R*)-configured amines in the second reductive step. Structures of the alcohol substrates explored in this study are shown below the schematic catalytic cycle. Me, methyl; Et, ethyl. See (*27*) for detailed structural representations of the alcohol substrates.

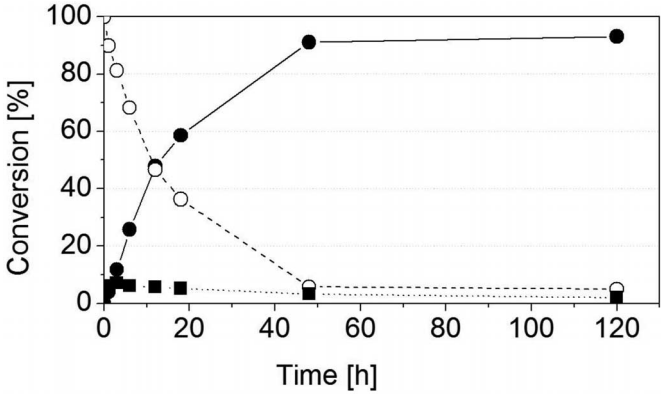

Fig. 2. Kinetics of asymmetric hydrogen-borrowing biocatalytic amination. The reaction of (*S*)-**1a** (20 mM) gives inverted (*R*)-**3a** using AA-ADH and Ph-AmDH with catalytic NAD^+ (1 mM; 5 mol %). Concentrations of the amine product (solid line, black circles), ketone intermediate (dotted line, black squares), and alcohol substrate (dashed line, white circles) were monitored over time. As expected, the concentration of the ketone intermediate **2a** remained constant and below the concentration of the nicotinamide coenzyme. See (*27*) for details.

with the AmDH in the amination step for the oxidation of the NADH, leading to accumulation of **2a** (*27*) (fig. S3). Therefore, the LBv-ADH was purified by ion exchange chromatography and size exclusion chromatography and was then recombined with the purified His-tagged Ph-AmDH for the alcohol amination reaction (**1a** concentration 20 mM, NAD^+ 5 mol %). Under these conditions, the concentration of the ketone **2a** at the end of the reaction was between 1.6 and 2.9% (less than the maximum theoretical value of 5%). Unfortunately, the final concentration of the amine product **3a** was also very low (<1%) (table S3). Replacing LBv-ADH with AA-ADH for the amination of (*S*)-**1a** led to the same results.

During the course of these preliminary experiments, we noticed that solutions containing the ADH (LBv-ADH or AA-ADH) together with the His-tagged Ph-AmDH tended to become cloudy after a few minutes of the reaction, generating an enzyme precipitate. However, no precipitation occurred even after more than 24 hours when the ADHs and the His-tagged Ph-AmDH were separately incubated in the same buffer under the same conditions. AA-ADH and LBv-ADH belong to the family of the short-chain dehydrogenases/reductases (SDRs). Both ADHs are homotetramers and possess the characteristic Ser-Tyr-Lys catalytic triad of the SDRs. Additionally, the LBv-ADH has two Mg^{2+} sites that are placed at the interphase between the monomeric units and are crucial for its stability (*25*). Although the crystal structure of AA-ADH was reported without an evident metal ion, a high homolog was crystallized in a stable form with six additional divalent cations (*28*). Furthermore, we noticed that the stability of LBv-ADH was significantly improved during purification when Mg^{2+} was added into the buffer, indicating a reversible dissociation process of the cation from the enzyme (*27*). Therefore, we speculated that enzyme precipitation in the dual-enzyme cascade might have been caused by coordination of free divalent cations, coming from the ADHs, to the His-terminal tag of the Ph-AmDH. As a consequence, enzyme aggregation and precipitation occurred. We then used a highly selective recombinant thrombin to cleave the His tag from the Ph-AmDH (*27*) (fig. S7). Incubation of the two purified ADHs with the Ph-AmDH devoid of a His tag resulted in visually more stable systems wherein enzyme aggregation and precipitation were not observed even after 24 hours.

The hydrogen-borrowing cascade was then repeated by combining AA-ADH with the Ph-AmDH (devoid of His tag) in ammonium chloride buffer at pH 8.7. AA-ADH is selective for (*S*)-**1a**, whereas Ph-AmDH shows (*R*)-selectivity in the reduction of the intermediate **2a**; hence, the overall cascade was expected to proceed with inversion of configuration. The reaction was tested at various concentrations of ammonium ions to ascertain the impact on the conversion. Under reaction conditions of (*S*)-**1a** = 20 mM, NAD^+ = 1 mM, and NH_4^+/NH_3 = 2 M, the conversion of alcohol to amine reached 85% after 24 hours, with an enantiomeric excess (ee) of >99% (*R*) (table S4).

Table 1. Asymmetric hydrogen-borrowing amination of enantiopure aromatic secondary alcohols 1a to 1n. Reactions were carried out at 30°C for 48 hours. See (*27*) for experimental details.

Amination of aromatic chiral secondary alcohols 1a to 1n with inversion of configuration				Amination of aromatic chiral secondary alcohols 1a to 1n with retention of configuration				Asymmetric amination of aromatic racemic secondary alcohols 1a to 1n			
Entry	Substrate	Conversion (%)	ee (%)	Entry	Substrate	Conversion (%)	ee (%)	Entry	Substrate	Conversion (%)	ee (%)
1	(*S*)-**1a**	95	>99(*R*)	15	(*R*)-**1a**	93	>99(*R*)	29	Rac-**1a**	81	>99(*R*)
2	(*S*)-**1b**	93	>99(*R*)	16	(*R*)-**1b**	36	>99(*R*)	30	Rac-**1b**	66	>99(*R*)
3	(*S*)-**1c**	55	97(*R*)	17	(*R*)-**1c**	27	97(*R*)	31	Rac-**1c**	47	97(*R*)
4	(*S*)-**1d**	65	>99(*R*)	18	(*R*)-**1d**	24	>99(*R*)	32	Rac-**1d**	78	>99(*R*)
5	(*S*)-**1e**	31	82(*R*)	19	(*R*)-**1e**	14	82(*R*)	33	Rac-**1e**	30	82(*R*)
6	(*S*)-**1f**	80	>99(*R*)	20	(*R*)-**1f**	85	>99(*R*)	34	Rac-**1f**	87	>99(*R*)
7	(*S*)-**1g**	92	82(*R*)	21	(*R*)-**1g**	92	83(*R*)	35	Rac-**1g**	92	83(*R*)
8	(*S*)-**1h**	96	>99(*R*)	22	(*R*)-**1h**	94	>99(*R*)	36	Rac-**1h**	84	>99(*R*)
9	(*S*)-**1i**	17	>99(*R*)	23	(*R*)-**1i**	30	>99(*R*)	37	Rac-**1i**	16	>99(*R*)
10	(*S*)-**1j**	14	>99(*R*)	24	(*R*)-**1j**	17	>99(*R*)	38	Rac-**1j**	16	>99(*R*)
11	(*S*)-**1k**	26	>99(*R*)	25	(*R*)-**1k**	33	>99(*R*)	39	Rac-**1k**	20	>99(*R*)
12	(*S*)-**1l**	12	>99(*R*)	26	(*R*)-**1l**	18	>99(*R*)	40	Rac-**1l**	12	>99(*R*)
13	(*S*)-**1m**	14	>99(*R*)	27	(*R*)-**1m**	27	>99(*R*)	41	Rac-**1m**	19	>99(*R*)
14	(*S*)-**1n**	7	>99(*R*)	28	(*R*)-**1n**	14	>99(*R*)	42	Rac-**1n**	9	>99(*R*)

Table 2. Asymmetric hydrogen-borrowing amination of aliphatic secondary alcohols 1o to 1s. Reactions were carried out at 30°C for 48 hours. See (*27*) for experimental details.

Amination of aliphatic chiral secondary alcohols with inversion of configuration				Amination of aliphatic chiral secondary alcohols with retention of configuration				Asymmetric amination of aliphatic racemic secondary alcohols			
Entry	Substrate	Conversion (%)	ee (%)	Entry	Substrate	Conversion (%)	ee (%)	Entry	Substrate	Conversion (%)	ee (%)
1	(*S*)-**1o**	94	99(*R*)	6	(*R*)-**1o**	91	>99(*R*)	11	Rac-**1o**	93	99(*R*)
2	(*S*)-**1p**	95	99(*R*)	7	(*R*)-**1p**	79	99(*R*)	12	Rac-**1p**	96	99(*R*)
3	(*S*)-**1q**	95	>99(*R*)	8	(*R*)-**1q**	83	>99(*R*)	13	Rac-**1q**	95	>99(*R*)
4	(*S*)-**1r**	74	>99(*R*)	9	(*R*)-**1r**	73	>99(*R*)	14	Rac-**1r**	66	>99(*R*)
5	(*S*)-**1s**	88	99(*R*)	10	(*R*)-**1s**	80	99(*R*)	15	Rac-**1s**	80	>99(*R*)

Monitoring the progress of the reaction revealed a maximum conversion in excess of 93% after 3 days (Fig. 2 and table S5). Increasing the concentration of ammonia up to 4 M led to a slight increase in conversion (95%; Table 1, entry 1, and tables S6 to S8). Addition of further aliquots of AA-ADH, Ph-AmDH, and NAD^+ after 2 days gave no further increase in conversion, indicating that the thermodynamic equilibrium had been reached. For improved catalytic efficiency of the cascade, the concentration of NAD^+ was reduced by a factor of 5, to 0.2 mM (1 mol %), which resulted in a slight drop in conversion to 76% (table S5 and figs. S9 and S10).

Surprisingly, when the same reaction conditions were applied to the amination of (*R*)-**1a** (20 mM) using LBv-ADH with the Ph-AmDH (minus His tag), the conversion to amine was <4% (table S9). We speculated that the instability of the LBv-ADH in ammonium chloride buffer at pH 8.7 might be the origin of the low conversion, so we investigated lower pH values. For ammonium chloride buffers, pH values of <8.5 cannot be attained; hence, ammonium formate buffer was investigated at various pH values (*29*). At pH 8 to 8.5, the amination of (*R*)-**1a** (20 mM) was achieved in 93% conversion and >99% ee (Table 1, entry 15). The cascade was then run by combining both of the stereocomplementary ADHs with the Ph-AmDH in one pot for the asymmetric amination of racemic **1a**, affording (*R*)-**3a** in >99% ee and 81% conversion (Table 1, entry 29).

The hydrogen-borrowing cascade was initially tested on a limited number of 1-phenyl-2-propanol derivatives **1a** to **1e** (Table 1) for amination with inversion of configuration (entries 1 to 5), retention of configuration (entries 15 to 19), and asymmetric amination of racemic alcohols (entries 29 to 33). Conversion varied from moderate to excellent, whereas the ee was excellent in almost all cases.

Whereas ADHs generally possess broad substrate specificity, the Ph-AmDH accepts solely phenylacetone and phenylacetaldehyde derivatives with elevated turnover numbers. Nonetheless, the generation of chimeric enzymes through domain shuffling from different parents can rapidly lead to new enzymes with increased activity or different and extended substrate specificity. The amino acid sequence of a stable chimeric AmDH (Ch1-AmDH) was recently published, although its substrate scope and stereoselectivity have not been elucidated (*30*). Thus, the Ch1-AmDH devoid of His tag was combined with the previously selected ADHs for the amination of a much broader panel of alcohols **1f** to **1s**. Aromatic substrates **1f** to **1h** bearing the phenyl ring in the α position (Table 1, entries 6, 20, and 34) and β position (Table 1, entries 7, 8, 21, 22, 35, and 36), relative to the secondary alcohol, as well as phenylethanol derivatives **1i** to **1n** with substituents in the ortho-, meta-, and para- positions (Table 1, entries 9 to 14, 23 to 28, and 37 to 42), were aminated with 99% ee (*R*) and conversions ranging from moderate to high. The only exception was alcohol **1g**, which was aminated with lower enantioselectivity (82 or 83% ee; Table 1, entries 7, 21, and 35). For this particular substrate, the progress of ee was monitored as a function of time (table S14 and fig. S12). The enantiomeric excess of amine **3g** remained constant, demonstrating that longer incubation times are not detrimental to the stereoselective outcome of the process. All the aliphatic secondary alcohols **1o** to **1s** examined (medium, long, and branched chain) were aminated with perfect ee and high conversions up to 96% (Table 2).

Table 3. Hydrogen-borrowing amination of primary alcohols 1t to 1z. Reactions were carried out at 30°C for 48 hours. See (*27*) for experimental details.

Entry	Substrate	Conversion (%)
1	**1t**	8
2	**1u**	99
3	**1v**	99
4	**1w**	99
5	**1x**	99
6	**1y**	61
7	**1z**	10

The hydrogen-borrowing amination is an extremely efficient and valuable method for the generation of optically active amines from alcohols. However, achiral terminal primary amines are also in high demand by the chemical industry, especially for the production of polymers and plasticizing agents (*1*). To demonstrate the broad applicability of the methodology, the amination of different primary alcohols was accomplished by combining the primary hT-ADH from *Bacillus stearothermophilus* (*31*) with either the Ch1-AmDH (Table 3, entries 1 to 6) or the Ph-AmDH (Table 3, entry 7). Quantitative conversion to the amine product was obtained with alcohols **1u** to **1x**.

To demonstrate the practical application of the methodology, we carried out bioaminations of five representative substrates—one for each structural category reported in Fig. 1—at a preparative scale. Starting from (*S*)-**1a** as the alcohol substrate, the conversion into the amine product (*R*)-**3a** reached 93% after 48 hours. The work-up consisted of extraction of the unreacted alcohol and ketone intermediate under acidic conditions, followed by the extraction of the amine product under basic conditions (*27*). The isolated yield of pure (*R*)-**3a** was 85% (99% ee). Following the same protocol, substrates (*S*)-**1g**, (*S*)-**1i**, (*S*)-**1q**, and **1u** were converted to the corresponding amines with 89%, 31%, 95%, and >99% conversion, respectively. The isolated yields of pure (*R*)-**3g**, (*R*)-**3i**, (*R*)-**3q**, and **3u** were 78%, 30%, 91%, and 91%, respectively. The enantiomeric excesses remained the same as for the experiments on an analytical scale.

Our dual-enzyme hydrogen-borrowing process enables the asymmetric amination of a broad range of secondary alcohols to afford the corresponding (*R*)-configured amines in high enantiomeric excess. Furthermore, in the majority of the cases, amination of primary alcohols proceeded in quantitative conversion. The biocatalytic system uses ammonia as the simplest amine donor and generates water as the sole innocuous byproduct. Ongoing studies are currently aimed at extending the substrate scope of the cascade through further protein engineering of AmDHs capable of aminating a wide range of more complex alcohols with elevated stereoselectivity. Although only enantiopure (*R*)-configured amines have been generated to date, the engineering of stereocomplementary AmDHs (*S*-selective) starting from D-amino acid dehydrogenases as scaffolds will complement the scope of our hydrogen-borrowing process. Finally, the use of lower concentrations of ammonia may be possible by the addition of further enzymes to derivatize the amine products and hence provide a thermodynamic driving force for the amination step.

REFERENCES AND NOTES

1. H. A. Wittcoff, B. G. Rueben, J. S. Plotkin, *Industrial Organic Chemicals* (Wiley- Interscience, New York, ed. 2, 2004).
2. T. C. Nugent, Ed., *Chiral Amine Synthesis* (Wiley-VCH, Weinheim, Germany, 2010).
3. E. Fabiano, B. T. Golding, M. M. Sadeghi, *Synthesis* **1987**, 190–191 (1987).
4. H.-J. Arpe, *Industrial Organic Chemistry* (Wiley-VCH, Weinheim, Germany, ed. 5, 2010).
5. F. Balkenhohl, K. Ditrich, B. Hauer, W. Ladner, *J. Prakt. Chem.* **339**, 381–384 (1997).
6. D. I. Sterling, in *Chirality in Industry*, A. N. Collins, G. N. Sheldrake, J. Crosby, Eds. (Wiley, Chichester, UK, 1992), pp. 209–222.
7. C. K. Savile *et al*., *Science* **329**, 305–309 (2010).
8. J. H. Schrittwieser, J. Sattler, V. Resch, F. G. Mutti, W. Kroutil, *Curr. Opin. Chem. Biol.* **15**, 249–256 (2011).
9. R. A. Sheldon, I. W. C. E. Arends, U. Hanefeld, *Green Chemistry and Catalysis* (Wiley-VCH, Weinheim, Germany, 2007).
10. T. Knaus, F. G. Mutti, L. D. Humphreys, N. J. Turner, N. S. Scrutton, *Org. Biomol. Chem.* **13**, 223–233 (2015).
11. S. Imm *et al*., *Angew. Chem. Int. Ed.* **50**, 7599–7603 (2011).
12. Y. Zhang, C.-S. Lim, D. S. B. Sim, H.-J. Pan, Y. Zhao, *Angew. Chem. Int. Ed.* **126**, 1423–1427 (2014).
13. The amination with the Ru catalyst (*7*) requires 3 mol % of the metal catalyst, 150°C, ammonia gas under pressure and inert atmosphere; racemic amines are obtained. The amination with Ir catalyst (*8*) requires 5 mol % of the metal catalyst coordinated to an expensive chiral ligand, 10 mol % of binaphthalene phosphoric acid as cocatalyst; *para*-anisidine is the nitrogen source; at least 33% of the alcohol starting material is wasted.
14. N. J. Oldenhuis, V. M. Dong, Z. Guan, *J. Am. Chem. Soc.* **136**, 12548–12551 (2014).
15. J. H. Sattler *et al*., *Angew. Chem. Int. Ed.* **51**, 9156–9159 (2012).
16. When using (*R*)-selective ω-TAs, D-alanine must be used. D-alanine has a high cost and, moreover, a D-alanine dehydrogenase is not known. Only L-alanine would be produced during the reaction. Hence, in the case of (*R*)-selective ω-TAs, the system works via removal rather than recycling of the pyruvate.
17. V. Resch, W. M. F. Fabian, W. Kroutil, *Adv. Synth. Catal.* **352**, 993–997 (2010).
18. M. J. Abrahamson, J. W. Wong, A. S. Bommarius, *Adv. Synth. Catal.* **355**, 1780–1786 (2013).
19. M. J. Abrahamson, E. Vázquez-Figueroa, N. B. Woodall, J. C. Moore, A. S. Bommarius, *Angew. Chem. Int. Ed.* **51**, 3969–3972 (2012).
20. S. K. Au, B. R. Bommarius, A. S. Bommarius, *ACS Catal.* **4**, 4021–4026 (2014).
21. M. M. Musa, R. S. Phillips, *Catal. Sci. Technol.* **1**, 1311–1323 (2011).
22. H. W. Höffken *et al*., *Biochemistry* **45**, 82–93 (2006).
23. The wild-type *Lactobacillus brevis* ADH is a NADP-dependent ADH. This enzyme was previously engineered to accept NAD as cofactor, and this variant was applied in this study.
24. W. Hummel, B. Riebel, PCT Int. Appl. WO 9947684 (1999).

25. N. H. Schlieben *et al.*, *J. Mol. Biol.* **349**, 801–813 (2005).
26. K. Tauber *et al.*, *Chemistry* **19**, 4030–4035 (2013).
27. See supplementary materials on *Science* Online.
28. A. C. Price, Y.-M. Zhang, C. O. Rock, S. W. White, *Structure* **12**, 417–428 (2004).
29. The Ph-AmDH tolerates different buffers well (i.e., ammonium chloride, formate, borate, citrate, acetate, oxalate). However, the homotetrameric LBv-ADHs contains two Mg^{2+} centers; therefore, strong chelators such as oxalate, citrate, and acetate must be avoided as buffer salts. Removal of these Mg^{2+} ions inactivates the enzyme (*32*).
30. B. R. Bommarius, M. Schürmann, A. S. Bommarius, *Chem. Commun.* **50**, 14953–14955 (2014).
31. R. Cannio, M. Rossi, S. Bartolucci, *Eur. J. Biochem.* **222**, 345–352 (1994).
32. K. Niefind, J. Müller, B. Riebel, W. Hummel, D. Schomburg, *J. Mol. Biol.* **327**, 317–328 (2003).

ACKNOWLEDGMENTS

The research leading to these results received funding from the European Union's Seventh Framework Programme FP7/2007-2013 under grant agreement 266025 (BIONEXGEN). The project leading to this application has received funding from the European Research Council under the European Union's Horizon 2020 research and innovation program (grant agreement no. 638271, BioSusAmin). T.K. and N.S.S. received funding from UK Biotechnology and Biological Sciences Research Council (BBSRC; BB/K0017802/1). N.J.T. is grateful to the Royal Society for a Wolfson Research Merit Award. Some aspects of the results reported here are the subject of a provisional patent application. Author contributions: F.G.M. and N.J.T. conceived the project and wrote the manuscript; F.G.M. planned the experiments, expressed and purified the AmDHs, performed the biocatalytic reactions, and analyzed the data; T.K. performed the gene cloning of all AmDHs and purified the ADHs; N.S.S. and M.B. provided intellectual and technical support; and M.B. and BASF provided the ADHs. We thank R. Heath for a preliminary kinetic assay of the Ph-AmDH.

SUPPLEMENTARY MATERIALS

www.sciencemag.org/content/349/6255/1525/suppl/DC1
Materials and Methods
Figs. S1 to S12
Tables S1 to S20
References (*33*–*36*)

30 June 2015; accepted 14 August 2015
10.1126/science.aac9283

BATTERIES

Alkaline quinone flow battery

Kaixiang Lin,[1] Qing Chen,[2] Michael R. Gerhardt,[2] Liuchuan Tong,[1] Sang Bok Kim,[1] Louise Eisenach,[3] Alvaro W. Valle,[3] David Hardee,[1] Roy G. Gordon,[1,2]* Michael J. Aziz,[2]* Michael P. Marshak[1,2]*

Storage of photovoltaic and wind electricity in batteries could solve the mismatch problem between the intermittent supply of these renewable resources and variable demand. Flow batteries permit more economical long-duration discharge than solid-electrode batteries by using liquid electrolytes stored outside of the battery. We report an alkaline flow battery based on redox-active organic molecules that are composed entirely of Earth-abundant elements and are nontoxic, nonflammable, and safe for use in residential and commercial environments. The battery operates efficiently with high power density near room temperature. These results demonstrate the stability and performance of redox-active organic molecules in alkaline flow batteries, potentially enabling cost-effective stationary storage of renewable energy.

The cost of photovoltaic (PV) and wind electricity has dropped so much that one of the largest barriers to getting most of our electricity from these renewable sources is their intermittency (*1*–*3*). Batteries provide a means to store electrical energy; however, traditional, enclosed batteries maintain discharge at peak power for far too short a duration to adequately regulate wind or solar power output (*1*, *2*). In contrast, flow batteries can independently scale the power and energy components of the system by storing the electro-active species outside the battery container itself (*3*–*5*). In a flow battery, the power is generated in a device resembling a fuel cell, which contains electrodes separated by an ion-permeable membrane. Liquid solutions of redox-active species are pumped into the cell, where they can be charged and discharged, before being returned to storage in an external storage tank. Scaling the amount of energy to be stored thus involves simply making larger tanks (Fig. 1A). Existing flow batteries are based on metal ions in acidic solution, but challenges with corrosivity, hydrogen evolution, kinetics, materials cost and abundance, and efficiency thus far have prevented large-scale commercialization. The use of anthraquinones in an acidic aqueous flow battery can dramatically

[1]Department of Chemistry and Chemical Biology, Harvard University, 12 Oxford Street, Cambridge, MA 02138, USA. [2]Harvard John A. Paulson School of Engineering and Applied Sciences, 29 Oxford Street, Cambridge, MA 02138, USA. [3]Harvard College, Cambridge, MA 02138, USA.
*Corresponding author. E-mail: aziz@seas.harvard.edu (M.J.A.); gordon@chemistry.harvard.edu (R.G.G.); michael.marshak@colorado.edu (M.P.M.)

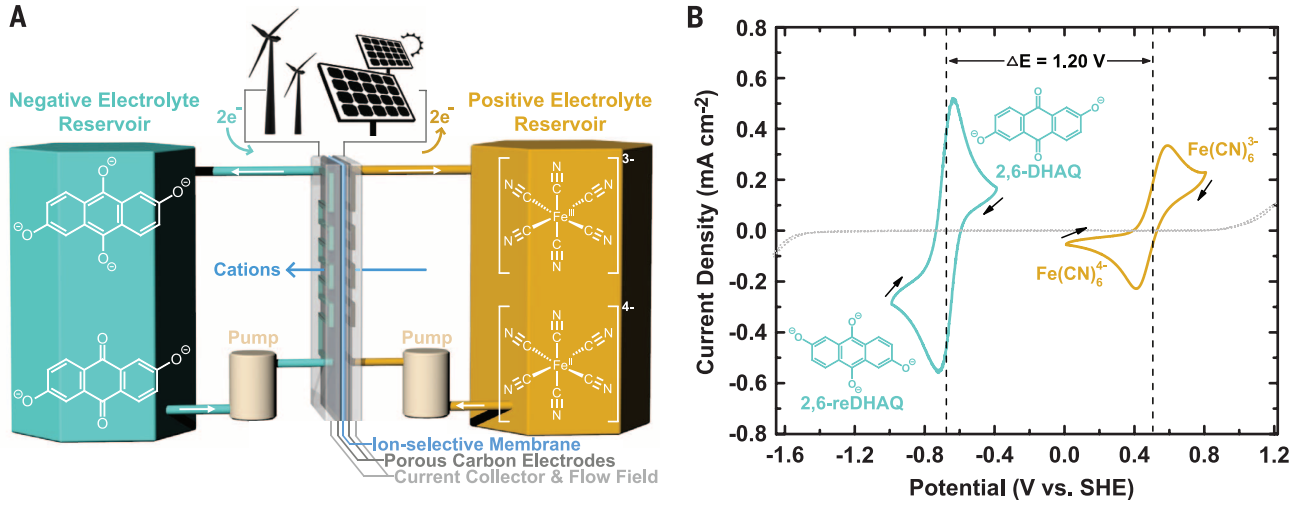

Fig. 1. Cyclic voltammetry of electrolyte and cell schematic. (**A**) Schematic of cell in charge mode. Cartoon on top of the cell represents sources of electrical energy from wind and solar. Curved arrows indicate direction of electron flow and white arrows indicate electrolyte solution flow. Blue arrow indicates migration of cations across the membrane. Essential components of electrochemical cells are labeled with color-coded lines and text. The molecular structures of oxidized and reduced species are shown on corresponding reservoirs. (**B**) Cyclic voltammogram of 2 mM 2,6-DHAQ (dark cyan curve) and ferrocyanide (gold curve) scanned at 100 mV/s on glassy carbon electrode; arrows indicate scan direction. Dotted line represents CV of 1 M KOH background scanned at 100 mV/s on graphite foil electrode.

Conversion of alcohols to enantiopure amines through dual-enzyme hydrogen-borrowing cascades

Francesco G. Mutti *et al.*

Science **349**, 1525 (2015);
DOI: 10.1126/science.aac9283